Council on Tall Buildings and Urban Habitat Korea

International Journal of
High-Rise Buildings
www.ctbuh-korea.org/ijhrb/index.php

International Journal of High-Rise Buildings
September 2024, Vol 13, No 3, 233-237
https://doi.org/10.21022/IJHRB.2024.13.3.233

Visco-elastically Connected Shear-flexural Structural System and Its Combination with Inter-story Isolation

Yang Xiang[1,2†], Lisa Liao[1], Meng Wang[3], and Guo-Qiang Li[1,2]

[1]*Department of Structural Engineering, Tongji University, China*
[2]*State Key Laboratory of Disaster Reduction in Civil Engineering, Tongji University, China*
[3]*Faculty of Architecture, Civil and Transportation Engineering, Beijing University of Technology, China.*

Abstract The proposal of viscoelastic shear-flexural structure with inter-story isolation (termed as VeSF-ISI structure) is to optimize the following problems of a traditional viscoelastic shear-flexural (VeSF) structure: (1) amplified inter-story drift of the shear-type subsystem; (2) construction difficulty in the installation of viscoelastic connection (VEC) on every story. By adopting the inter-story isolation (ISI), above problems are solved and other structural benefits are revealed. Furthermore, this paper explores the feasible configuration, dynamic property and seismic response of a 20-story VeSF-ISI structure. The results of numerical analysis suggest that: (1) the VeSF-ISI structure has well-controlled seismic responses, especially in terms of the inter-story drift and base moment; (2) the average energy dissipation of VECs is 3.7 times more than that of a VeSF structure; (3) when the ISI is set in the lower story, the acceleration of the flexural-type subsystem is better controlled and the influence on the shear-type subsystem is moderate.

Keywords High-rise structure, Shear-flexural structure, Viscoelastic link, Inter-story drift mitigation, Inter-story isolation

†Corresponding author:
Yang Xiang
E-mail:
y_xiang@tongji.edu.cn

1. Introduction

The concept of using deformable connection to connect adjacent structures (Raheem, 2014, Zhang and Xu, 1999) or subsystems in a structure (Dubina et al., 2008, Greco and Marano, 2016) is an increasing trend around the world. It limits the transmission of inertial forces between dynamically dissimilar structural systems, dissipates vibration energy by flexible connections, and reduce the overall responses of the system. According to this concept, many kinds of passive dampers are proposed, including friction damper (Ng and Xu, 2006), fluid damper (Xu et al., 2003, Yang et al., 2003), viscoelastic damper (Kim et al., 2006, Tubaldi, 2015), and metallic damper (Chan and Albermani, 2008). These researches proved the effectiveness of damper-linked system both experimentally and numerically.

Except for structural efficiency, architectural aesthetics and functionality of these damper-linked structures are also important. To achieve multiple goals, an innovative floor anchorage system has been developed (Tsampras et al., 2016, Fleischman et al., 2015). The ductile anchorage connector was underneath the floor diaphragm, which is low-invasive to the building, and reduced the inertial forces. In compliance with similar configurations, the research about seismic responses of steel concentrically braced frame with floor sliding friction dampers was studied by Paronesso and Lignos (Paronesso and Lignos, 2022). Besides, a space-compact viscoelastic shear-flexural (VeSF) structure, was proposed by Xiang et al. (Xiang et al., 2023). This VeSF structure used viscoelastic connection (VEC) on every story to link the shear- and flexural-type subsystems and presented 20%~40% reduction on acceleration according to the computation. However, several noted or potential problems remain unresolved: (1) the inter-story drift of the shear-type subsystem is amplified; (2) the construction difficulty in the installation of dampers on every story; (3) the low efficiency in dissipate capacity of VECs equipped in stories with small drifts.

To tackle the above-mentioned issues, the inter-story isolation (ISI) is utilized. Inter-story isolation (also known as intermediate or mid-story isolation) is a popular method for aseismic building design and retrofit (Warn and Ryan, 2012, Zhu et al., 2023). The numerical analysis proved that with appropriate design, the seismic response of upper part (stories above ISI) can be mitigated. Considering the benefit of reduced seismic demands on the substructures, in this study, a new structure to optimize the VeSF structure by incorporating the intermediate isolation is proposed. A feasible configuration of a VeSF-ISI structure is given in Section 2. And three multi-degree-of-freedom (MDOF) models are analyzed in Section 3: a VeSF-ISI structure, a VeSF structure, and a conventional shear-flexural structure. In Section 4, structural responses of three structures and the relevant approach

are elaborated. Main conclusions are given in Section 5.

2. Structural Configuration

The viscoelastic shear-flexural structure with inter-story isolations (VeSF-ISI) contains both characteristics of the inter-story isolation and the viscoelastic connection. To be specific, a VeSF-ISI structure contains a shear-type lateral-force resisting subsystem (e.g. steel frame) and a flexural-type lateral-force resisting subsystem (e.g. RC core, shear wall, et al.), and intermediate isolations are set in a certain story of the former subsystem. In the US, the connections between subsystems are VECs while in the LS, two subsystems are linked rigidly.

A feasible actualization of a VeSF-ISI structure is presented in Figure 1. Plotted in Figure 1(a) is the elevation of a 20-story VeSF-ISI structure, including a frame and a core as its subsystems. Figure 1(b) and (c) show the classic actualization and configuration of inter-story isolation (ISI) layer. The height of the ISI story is smaller than that of other stories. Figure 1(d) and (e) depict how the shear- and flexural-type subsystems are decoupled by VEC.

3. Mechanical Model

In this section, three multi-degree of freedom (MDOF) models are adopted to explore the benefits of a VeSF-ISI. A typical 20-story VeSF-ISI structure is modeled in Figure 2(a), with the inter-story isolation (ISI) layer set between the 15th and the 16th story. Shear springs and flexural beams are used to represent the shear- and the flexural-type subsystems separately. The "spring & dashpot" elements are used to simulate the stiffness and damping of ISI and VEC. Another two MODF models are illustrated in Figure 2(b) and (c), representing a VeSF structure and a conventional shear-flexural structure respectively.

For the three models in Figure 2, subsystems have equal mass, being distributed uniformly along the height. On the j^{th} story, it contains 2 lumped masses: m_j and M_j, representing the mass of the flexural-type and the shear-type subsystem separately. The stiffness ratio of two subsystems (α) is calculated by the Equation (1):

$$\alpha = H\sqrt{\frac{G_e A}{EI}} \tag{1}$$

where H stands for total height of a structure (for this VeSF-ISI structure $H = 67.2$ m); G_eA and EI represent equivalent shear and bending modulus.

For brevity, this paper only presents matrixes of the VeSF-ISI structure modeled in Figure 2(a). In the LP, shear- and flexural-type subsystems are still connected rigidly while for the UP and the ISI story, subsystems are decoupled by VECs, which means that two DoFs are used per story to represent different lateral drifts of subsystems in the latter parts. The mass and stiffness matrix should be extended. The accordant mass matrix of this VeSF-ISI structure is calculated as below:

$$\mathbf{M}_{\text{VeSF-ISI}} = \mathbf{M}^{\text{flexu}}_{\text{VeSF-ISI}} + \mathbf{M}^{\text{shear}}_{\text{VeSF-ISI}} \tag{2}$$

$$\mathbf{M}_{\text{VeSF-ISI}} = \begin{bmatrix} m_1 + M_1 & & & & & & & & & & & & & & & & & & & \\ & m_2 + M_2 & & & & & & & & & & & & & & & & & \\ & & \cdots & & & & & & & & & & & & & & & & \\ & & & m_{15} + M_{15} & & & & & & & & & & & & & & & \\ & & & & m_{\text{ISI}} & & & & & & & & & & & & & & \\ & & & & & M_{\text{ISI}} & & & & & & & & & & & & & \\ & & & & & & m_{16} & & & & & & & & & & & & \\ & & & & & & & M_{16} & & & & & & & & & & & \\ & & & & & & & & \cdots & & & & & & & & & \\ & & & & & & & & & m_{20} & & & & & & & & \\ & & & & & & & & & & M_{20} & & & & & & & \end{bmatrix} \tag{3}$$

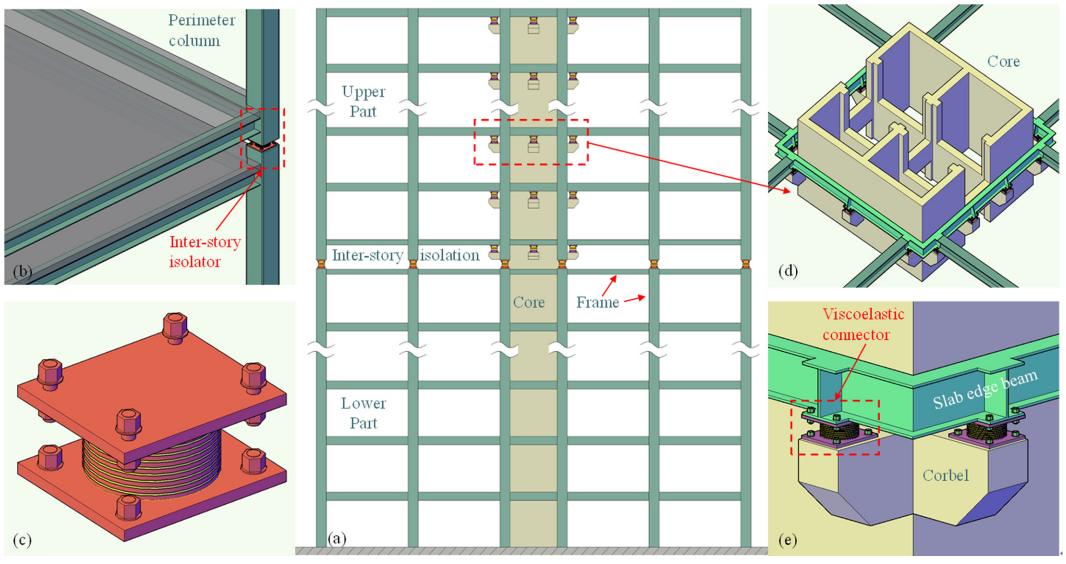


Fig. 1. A feasible actualization of a VeSF-ISI structure.

The overall stiffness matrix of the VeSF-ISI structure contains four parts?(1) stiffness of shear-type subsystem; (2) stiffness of flexural-type subsystem; (3) stiffness of viscoelastic connection (VEC); (4) stiffness of inter-story isolation (ISI), as detailed in the following Equation (4) ~ Eq. (6).

$$\mathbf{K}_{\text{VeSF-ISI}} = \mathbf{K}^{\text{shear}}_{\text{VeSF-ISI}} + \mathbf{K}^{\text{flexu}}_{\text{VeSF-ISI}} + \mathbf{K}^{\text{VEC}}_{\text{VeSF-ISI}} \tag{4}$$

$$\mathbf{K}^{\text{shear}}_{\text{VeSF-ISS}} = \begin{bmatrix} k_1^{\text{shear}} + k_2^{\text{shear}} & -k_2^{\text{shear}} & 0 & \cdots & 0 & 0 & 0 & 0 & 0 & \cdots & 0 & 0 \\ & k_2^{\text{shear}} + k_3^{\text{shear}} & -k_3^{\text{shear}} & \cdots & 0 & 0 & 0 & 0 & 0 & \cdots & 0 & 0 \\ & & \cdots & \cdots & \cdots & \cdots & \cdots & \cdots & \cdots & \cdots & \cdots & \cdots \\ & & & \cdots & -k_{\text{ISI}}^{\text{shear}} & 0 & 0 & 0 & 0 & \cdots & 0 & 0 \\ & & & & k_{\text{ISI}}^{\text{shear}} + k_{16}^{\text{shear}} & 0 & -k_{16}^{\text{shear}} & 0 & 0 & \cdots & 0 & 0 \\ & & & & & 0 & 0 & 0 & 0 & \cdots & 0 & 0 \\ & & & & & k_{16}^{\text{shear}} + k_{17}^{\text{shear}} & 0 & -k_{17}^{\text{shear}} & 0 & \cdots & 0 & 0 \\ & & & & & & 0 & 0 & 0 & \cdots & 0 & 0 \\ & & & & & & k_{17}^{\text{shear}} + k_{18}^{\text{shear}} & 0 & \cdots & 0 & 0 \\ & & & \text{sym} & & & & & \cdots & \cdots & \cdots \\ & & & & & & & & & 0 & 0 \\ & & & & & & & & & & k_{20}^{\text{shear}} \end{bmatrix} \tag{5}$$

$$\mathbf{K}^{\text{flexu}}_{\text{VeSF-ISS}} = \begin{bmatrix} k_{1,1}^{\text{flexu}} & k_{1,2}^{\text{flexu}} & \cdots & k_{1,15}^{\text{flexu}} & k_{1,16}^{\text{flexu}} & 0 & k_{1,17}^{\text{flexu}} & 0 & \cdots & k_{1,20}^{\text{flexu}} & 0 \\ & k_{2,2}^{\text{flexu}} & \cdots & k_{2,15}^{\text{flexu}} & k_{2,16}^{\text{flexu}} & 0 & k_{2,17}^{\text{flexu}} & 0 & \cdots & k_{2,20}^{\text{flexu}} & 0 \\ & & \cdots & \cdots & \cdots & \cdots & \cdots & \cdots & \cdots & \cdots & \cdots \\ & & & k_{15,15}^{\text{flexu}} & k_{15,16}^{\text{flexu}} & 0 & k_{15,17}^{\text{flexu}} & 0 & \cdots & k_{15,20}^{\text{flexu}} & 0 \\ & & & & k_{16,16}^{\text{flexu}} & 0 & k_{16,17}^{\text{flexu}} & 0 & \cdots & k_{16,20}^{\text{flexu}} & 0 \\ & & & & & 0 & 0 & 0 & \cdots & 0 & 0 \\ & & & & & & k_{17,17}^{\text{flexu}} & 0 & \cdots & k_{17,20}^{\text{flexu}} & 0 \\ & & & & & & & 0 & \cdots & 0 & 0 \\ & & & \text{sym} & & & & & \cdots & \cdots & \cdots \\ & & & & & & & & & k_{20,20}^{\text{flexu}} & 0 \\ & & & & & & & & & & 0 \end{bmatrix} \tag{6}$$

where $k_{p,j}^{\text{flexu}}$ is the lateral force of the j^{th} story when a unit drift at the p^{th} story is conducted in the flexural-type subsystem, $k_{\text{ISI}}^{\text{shear}}$ is the shear spring's stiffness of the j^{th} story. It is worth noting that $k_{\text{ISI}}^{\text{shear}}$ is the stiffness of the intermediate isolations. The intermediate isolations adopted in this paper is lead rubber bearing (LRB) with idealized force–deformation bilinear behavior. The force–deformation bilinear characteristics are: (1) initial stiffness $k_1 = 0.1k_{16}^{\text{shear}}$; (2) post yield stiffness $k_2 = 0.2k_1$; (3) yield strength $F_y = 0.05g\sum_{j=\beta}^{20} M_j$, g is the gravitational acceleration and β is the layer of the inter-story isolation; (4) characteristic strength $Q = f_y A_p$, wherein, f_y is the yield strength of lead core under shear and A_p denotes the lead core cross-sectional area. The global damping ($\mathrm{C}_{\text{VeSF-ISI}}$) of a VeSF-ISI structure is made up of two parts and can be calculated via Equation (7).

$$\mathbf{C}_{\text{VeSF-ISI}} = \mathbf{C}^{\text{Inherent}}_{\text{VeSF-ISI}} + \mathbf{C}^{\text{VEC}}_{\text{VeSF-ISI}} \tag{7}$$

It is worth mentioning that the $\mathbf{C}^{\text{Inherent}}_{\text{VeSF-ISI}}$ is expanded by the Rayleigh damping matrix of conventional structure. $\mathbf{C}^{\text{VEC}}_{\text{VeSF-ISI}}$ is the extra damping induced by the VECs. The stiffness k^{VEC} and the damping coefficient c^{VEC} of a VEC vary with the frequency (ω^{VEC}). To be brief, a nominal stiffness of the VEC is formulated by Equation (8).

$$k_{\text{nor,j}}^{\text{VEC}} = k_j^{\text{shear}} \cdot \kappa_j \tag{8}$$

where k_j is the nominal stiffness ratio between the VEC and the shear-type subsystem at j^{th} story. The mechanical model of the VEC used in this paper has been conducted experimentally and numerically by Xiang et al. (Xiang et al., 2021).

4. Structural Response Demonstration

4.1. Methodology for structural response analysis

A VeSF-ISI structure combines the mechanisms of viscoelastic connection (VEC) and inter-story isolation (ISI): one is using VEC to decouple the shear- (frame) and flexural-type (core) subsystems, the other is using ISI as a filter to limit inertial forces transmitting from the lower part (LP) to the upper part (UP). The dynamic equilibria of the VeSF-ISI structure are Equations (9)~(10).

$$\mathbf{M}_{\text{VeSF-ISI}}\{\ddot{x}_{\text{VeSF-ISI}}\} + \mathbf{C}_{\text{VeSF-ISI}}\{\dot{x}_{\text{VeSF-ISI}}\} + \mathbf{K}_{\text{VeSF-ISI}}\{x_{\text{VeSF-ISI}}\} = -\mathbf{M}_{\text{VeSF-ISI}}\{\iota\}\{a_g\} \tag{9}$$

$$\{x_{\text{VeSF-ISI}}\} = \left[x_1^{\text{flexu}} \;\; x_1^{\text{shear}} \;\; x_2^{\text{flexu}} \;\; x_2^{\text{shear}} \ldots \; x_{\text{ISI}}^{\text{flexu}} \;\; x_{\text{ISI}}^{\text{shear}} \ldots \; x_{20}^{\text{flexu}} \;\; x_{20}^{\text{shear}}\right]^{\text{T}} \tag{10}$$

Where $\{\iota\}$ is an influential vector with all elements equal to unity; $\{x_{\text{VeSF-ISI}}\}$ is the displacement matrix of the VeSF-ISI structure, x_j^{flexu} and x_j^{shear} are the drift of flexural- and shear-type subsystems on j^{th} story; $x_{\text{ISI}}^{\text{flexu}}$ and $x_{\text{ISI}}^{\text{shear}}$ represent the deformation of ISI; $\{a_g\}$ refers to the relative ground acceleration. In this paper, the Newmark-β method is used on the time history analysis on the Matlab platform.

4.2. Response comparison: different structures under a typical wave

In this section, under the 80% intensity of the El Centro wave, the seismic responses of three mentioned models are compared and the advantages of the VeSF-ISI structure are further demonstrated. Figure 3 draws peak seismic responses of three structures.

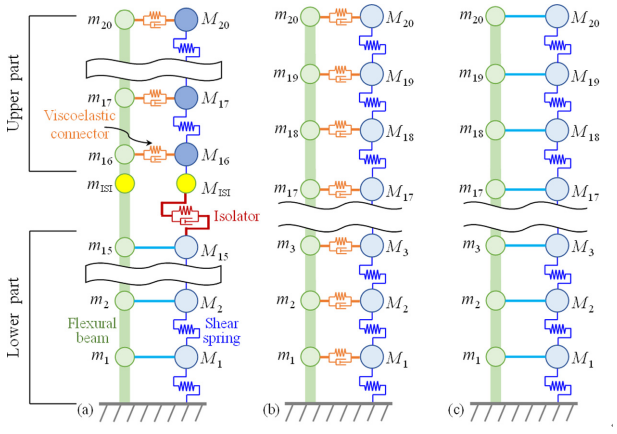


Fig. 2. MODF models: (a) VeSF-ISI structure; (b) VeSF structure; (c) Conventional shear-flexural structure.

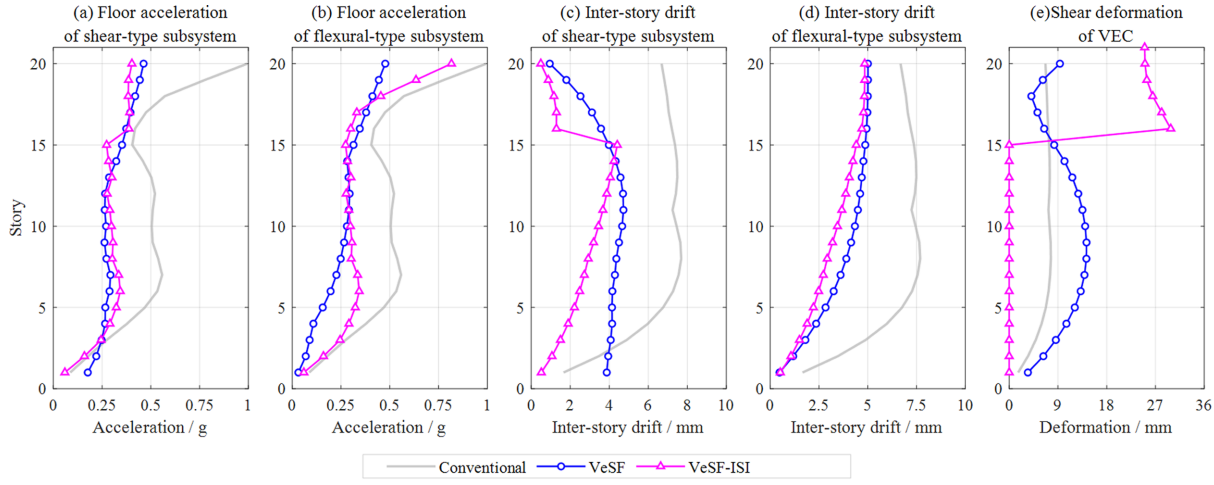


Fig. 3. Peak seismic response of different structures: (a), (b) Peak floor acceleration; (c), (d) Peak inter-story drift; (e) Peak shear deformation.

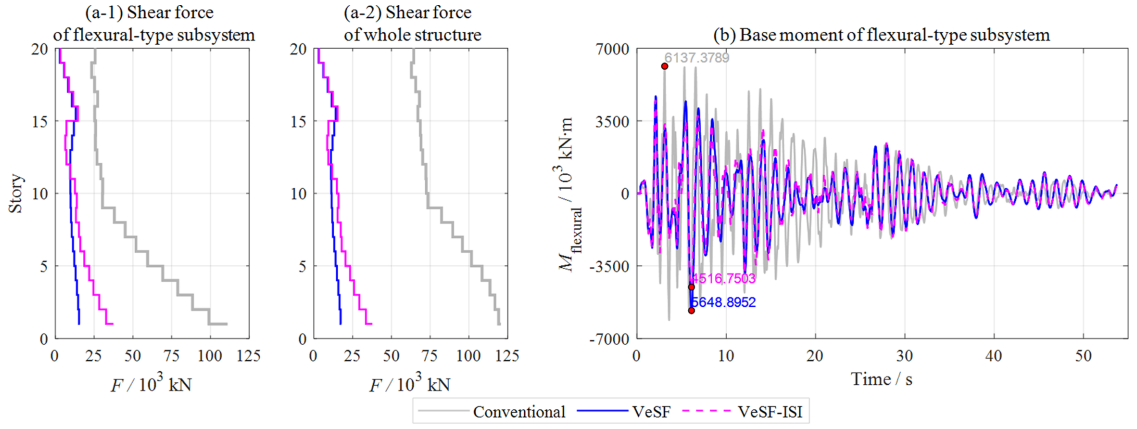


Fig. 4 (a-1), (a-2) Peak shear force; (b) Time history curve of the base moment.

From Figure 3(a), for the shear-type subsystem, the control for floor acceleration (with the reduction about 12%~27%) is obvious in the bottom and the top of the structure. It is due to the inter-story isolation (ISI) limit the transfer of the vibration from the lower part (LP) to the upper part (UP). From Figure 3(b), the PFA of the flexural-type subsystem in the VeSF-ISI structure is amplified, comparing to the VeSF structure. This is attributed to that in the latter structure, VECs are installed on every story and extra damping is introduced in the LP. However, the PFA still decreases as compared with the conventional structure.

From Figure 3(c) and (d), comparing to other two structures, the PISDs of the VeSF-ISI structure are greatly controlled, which reduces the possibility of frame yielding and core cracking. Noticeably, the inter-story drift reaches to the peak in the layer with ISI, which is slightly amplified compared to that of the VeSF structure. For the flexural-type subsystem, the deforming patterns of both the VeSF-ISI and the VeSF structure are similar, and there is a roughly 20% reduction on PISD compared to the VeSF structure from the 4th story to the 9th story.

From Figure 3(e), the VeSF-ISI structure has bigger shear deformation of VEC and it means VECs are activated to a greater extend. Comparing Figure 3(a)~(d), the VeSF-ISI structure shows better control in the PISD than the PFA and with regard to the conventional structure the VeSF-ISI structure has global advantages.

Plotted in Figure 4(a-1) and (a-2) are peak shear of three structure. Although the shear of the VeSF-ISI structure is increased with regard to that of the VeSF structure, it still remains in the well-controlled level (only 25% the number of the conventional counterpart). Figure 4(b) is the time history curve of the base moment in the flexural-type subsystem. It can be easily noticed that during the earthquake excitation, the VeSF-ISI structure has the lowest base moment, which reduce the design difficulty of the core.

5. Conclusions

The viscoelastic shear-flexural structure with inter-story isolation (VeSF-ISI), referring to set an inter-story

isolation (ISI) layer in the middle of the viscoelastic shear-flexural (VeSF) structure, not only solve problems like amplified inter-story drift and construction difficulty but also brings extra benefits: significant increase in the average energy dissipation capacity of VECs and reduction in the base moment of the flexural-type subsystem. Although the shear and the floor acceleration of the flexural subsystem are moderately amplified, the seismic responses are still in the low-level compared to the conventional shear-flexural structure.

Acknowledgments

This work is supported by the National Key Research and Development Program of China (No. 2022YFC 3801900, 2023YFC3806602) and the National Natural Science Foundation of China (No. 52308524). The financial supports are gratefully acknowledged.

References

CHAN, R. W. K. & ALBERMANI, F. (2008). Experimental study of steel slit damper for passive energy dissipation. Engineering Structures, 30, 1058-1066.

DUBINA, D., STRATAN, A. & DINU, F. (2008). Dual high-strength steel eccentrically braced frames with removable links. Earthquake Engineering & Structural Dynamics, 37, 1703-1720.

FLEISCHMAN, R., RESTREPO, J., NEMA, A., ZHANG, D. C., SHAKYA, U., ZHANG, Z., SAUSE, R., TSAMPRAS, G. & MONTI, G. (2015). Inertial Force-Limiting Anchorage System for Seismic Resistant Building Structures. Structures Congress, Apr 23-25 2015 Portland, OR. 1302-1313.

GRECO, R. & MARANO, G. C. (2016). Multi-objective optimization of a dissipative connection for seismic protection of wall-frame structures. Soil Dynamics and Earthquake Engineering, 87, 151-163.

KIM, J., RYU, J. & CHUNG, L. (2006). Seismic performance of structures connected by viscoelastic dampers. Engineering Structures, 28, 183-195.

NG, C. L. & XU, Y. L. (2006). Seismic response control of a building complex utilizing passive friction damper: Experimental investigation. Earthquake Engineering & Structural Dynamics, 35, 657-677.

PARONESSO, M. & LIGNOS, D. G. (2022). Seismic design and performance of steel concentrically braced frame buildings with dissipative floor connectors. Earthquake Engineering & Structural Dynamics, 51, 3505-3525.

RAHEEM, S. E. A. (2014). Mitigation measures for earthquake induced pounding effects on seismic performance of adjacent buildings. Bulletin of Earthquake Engineering, 12, 1705-1724.

TSAMPRAS, G., SAUSE, R., ZHANG, D., FLEISCHMAN, R. B., RESTREPO, J. I., MAR, D. & MAFFEI, J. (2016). Development of deformable connection for earthquake-resistant buildings to reduce floor accelerations and force responses. Earthquake Engineering & Structural Dynamics, 45, 1473-1494.

TUBALDI, E. (2015). Dynamic behavior of adjacent buildings connected by linear viscous/viscoelastic dampers. Structural Control & Health Monitoring, 22, 1086-1102.

WARN, G. P. & RYAN, K. L. (2012). A review of seismic isolation for buildings: Historical development and research needs. Buildings, 2, 300-325.

XIANG, Y., KOETAKA, Y. & NISHIRA, K. (2021). Steel frame with aseismic floor: From the viscoelastic decoupler model to the elastic structural response. Earthquake Engineering & Structural Dynamics, 50, 1651-1670.

XIANG, Y., WANG, M., SUN, F.-F. & LI, G.-Q. (2023). Aseismic high-rise structure with visco-elastically connected shear- and flexural-subsystems. Engineering Structures, 291.

XIANG, Y. & XIE, H. R. (2021). Probabilistic effectiveness of visco-elastic dampers considering earthquake excitation uncertainty and ambient temperature fluctuation. Engineering Structures, 226.

XU, Y. L., YANG, Z. & LU, X. L. (2003). Inelastic seismic response of adjacent buildings linked by fluid dampers. Structural Engineering and Mechanics, 15, 513-534.

YANG, Z., XU, Y. L. & LU, X. L. (2003). Experimental seismic study of adjacent buildings with fluid dampers. Journal of Structural Engineering-Asce, 129, 197-205.

ZHANG, W. S. & XU, Y. L. (1999). Dynamic characteristics and seismic response of adjacent buildings linked by discrete dampers. Earthquake Engineering & Structural Dynamics, 28, 1163-1185.

ZHU, Y. P., LANG, Z. Q., FUJITA, K. & TAKEWAKI, I. (2023). Analysis and design of non-linear seismic isolation systems for building structures-An overview. Frontiers in Built Environment, 8.